Communication

Critical Angle Formulation of Nonuniform Plane Waves for Determining Correct Refraction Angles at Planar Interface

Yongwan Kim, Hyunjun Yang, and Jungsuek Oh

***Abstract*—The expressions and properties of the critical angles of nonuniform plane waves for determining the correct refraction angle at the infinite planar interface of two linear, isotropic, and homogeneous media are presented. The two media could be lossless or lossy. For the case where the complex wave vector of Adler–Chu–Fano formulation and the normal vector to the interface are coplanar, a critical angle equation, which is simpler than the extant one, under the condition that one or two critical angles exist, is formulated. In addition, for the case where the complex wave vector and normal vector to the interface are noncoplanar, a critical angle equation is formulated, rendering the 3-D nonuniform plane wave refraction feasible for utilization in many areas of optics. The presented critical angle equations were validated for various nonuniform plane waves and media.**

***Index Terms*—Absorbing media, critical angle, deep penetration, inhomogeneous plane waves, nonuniform plane waves, optics, ray tracing.**

I. Introduction

The refraction of an electromagnetic (EM) plane wave on the infinite planar interface between possibly lossy media is a widely studied problem in optics and EM theory [1], [2], [3], [4], [5], [6], [7], [8], [9], [10], [11], which is used in a variety of areas, e.g., leaky-wave antenna, remote sensing, EM ray-tracing technique, material analysis/microscopy, interaction with biological tissues, and metasurface [9], [10], [11], [12], [13], [14], [15], [16], [17], [18]. When an incident uniform plane wave in a lossless medium impinges upon an infinite planar interface of a lossy medium, the application of Snell's law produces a refraction angle of complex value [19]. Furthermore, if this plane wave with a complex propagation angle impinges upon another planar interface, both incidence and refraction angles at the second interface may be complex-valued. The physical meaning of these complex-valued propagation angles is difficult to understand. The Adler–Chu–Fano formulation in [20] allows for a physically meaningful interpretation in this situation by keeping all angles as real values while separating the propagation vector into attenuation vector $\vec{\alpha}$ and phase vector $\vec{\beta}$, i.e., the complex propagation angle is converted into two real angles—equal attenuation angle ζ and phase angle ξ. Hence, the wave becomes a nonuniform plane wave [20]. Consequently, when a nonuniform plane wave impinges upon a planar interface, the incidence and refraction angles can be written as ζ_1 and ξ_1 and ζ_2 and ξ_2, respectively.

Manuscript received 1 August 2022; revised 16 November 2022; accepted 20 December 2022. Date of publication 9 January 2023; date of current version 6 March 2023. This work was supported by the Institute of Information and Communications Technology Planning and Evaluation (IITP) through the South Korea Government (MIST) under Grant 2019-0-00098 (Advanced and Integrated Software Development for Electromagnetic Analysis). *(Corresponding author: Jungsuek Oh.)*

The authors are with the Institute of New Media and Communications (INMC) and the Department of Electrical and Computer Engineering, Seoul National University, Seoul 08826, South Korea (e-mail: yongwankim@snu.ac.kr; guswns6217@snu.ac.kr; jungsuek@snu.ac.kr).

Color versions of one or more figures in this communication are available at https://doi.org/10.1109/TAP.2022.3233489.

Digital Object Identifier 10.1109/TAP.2022.3233489

Two types of critical angles exist for the refraction of nonuniform plane waves [20], [21], [22]. The first one is ξ_1^{ζ}, which is ξ_1 leading to $\zeta_2 = 90°$, and the second one is ξ_1^{ξ}, which is ξ_1 leading to $\xi_2 = 90°$. The determination of ζ_2 or ξ_2 when ξ_1 exceeds $\xi_1^{\zeta,\xi}$ may produce ambiguous results due to the multivalued function property of the inverse trigonometric function [20], [21], which means that, when $\xi_1 \in (\xi_1^{\zeta,\xi}, 90°]$, ζ_2 or ξ_2 can have two different values mathematically. ζ_2 or ξ_2 could be in the intervals $[0, 90°)$ or $(90°, 180°]$, i.e., nonmonotonic or monotonic behavior of ζ_2 or ξ_2 [21]. Roy et al. [20] and Frezza and Tedeschi [21] discovered the correct determination to be the monotonic behavior. Therefore, $\xi_1^{\zeta,\xi}$ must be calculated to determine the correct values of ζ_2 or ξ_2, which could be in the interval [0, 90°] or [90°, 180°].

For the case where the incidence propagation vectors $\vec{\alpha}_1$ and $\vec{\beta}_1$ and the unit vector normal to interface $\hat{z}$ are coplanar, i.e., a two-dimensional (2-D) case, an exact analytic expression of $\xi_1^{\zeta,\xi}$ was presented in [22]. In this study, however, we derive a simpler expression of $\xi_1^{\zeta,\xi}$ for the 2-D case, which is more efficient for areas requiring massive computations, such as the EM ray-tracing simulation. In addition, we present the conditions of the plane wave and media that produce one or two critical angles for the 2-D case with the interface between two possibly lossy media, further from [23], which thoroughly treated those conditions with the interface between lossless and lossy media to deal with practical applications of deep penetration condition. For the 3-D case, i.e., the case where $\vec{\alpha}_1$, $\vec{\beta}_1$, and $\hat{z}$ are noncoplanar, which is more common than the 2-D case, albeit more complex, no analytic expression of $\xi_1^{\zeta,\xi}$ has been presented yet. Consequently, the 3-D case of the refraction of nonuniform plane waves has not been applied to most areas utilizing the nonuniform plane wave theory, such as EM ray-tracing simulation and deep penetration condition analysis in lossy media [14], [15], [16], [22], [23], although it is the more general case between the two. In this study, an analytic expression and properties of $\xi_1^{\zeta,\xi}$ for the 3-D case are presented, rendering the 3-D nonuniform plane wave refraction feasible for utilization in many areas of optics. For the EM ray-tracing technique, it will lead to more accurate analysis results for complex penetrable structures. It can also be widely used to expand various EM theories related to nonuniform plane waves. For instance, for deep penetration condition theory, whose practical 2-D implementation in the real world is verified in [24] and which can be applied to numerous practical applications such as ground penetrating radar [25] and leaky-wave antenna for ultrahigh-field magnetic resonance imaging [26], our study could contribute to derive the effect caused by the transition from 2-D to 3-D condition.

II. Simple Critical Angle Formulation of 2-D Case

A. Critical Angle Formulation and Condition That One or Two Critical Angles Exist

Fig. 1 shows the incidence and refraction of nonuniform plane wave at the planar interface between two media for the 2-D case.

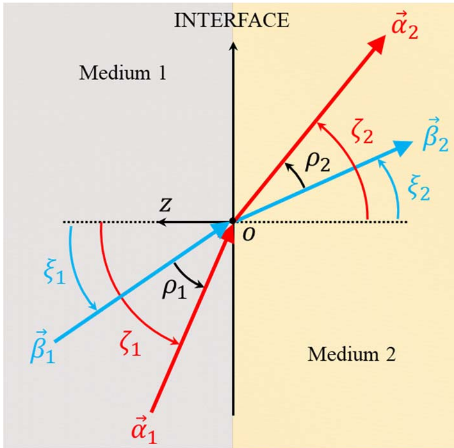

Fig. 1. Incidence and refraction of nonuniform plane wave on the planar interface between two isotropic homogeneous possibly lossy media when $\vec{\alpha}_1$ and $\vec{\beta}_1$ and the unit vector normal to the interface $\hat{z}$ are coplanar, i.e., 2-D case.

Frezza and Tedeschi [22] derived a critical angle formulation for the 2-D case with lossy first medium, which is presented as follows:

$$\xi_1^{\zeta,\xi} = \begin{cases} \tan^{-1}\left\{\dfrac{\tan\rho_1 \pm \sqrt{\tan^2\rho_1 - 4\chi(\chi-1)}}{2(\chi-1)}\right\}, & \chi \neq 1 \quad (1\text{-}1)\\ \tan^{-1}\left(\dfrac{1}{\tan\rho_1}\right), & \chi = 1 \quad (1\text{-}2)\end{cases}$$

where ρ_1 is described in Fig. 1, and $\chi = (\alpha_{02}\beta_{02})/(\alpha_{01}\beta_{01})$. α_{01} and β_{01}, and α_{02} and β_{02} are the intrinsic attenuation and phase constants of media 1 and 2, respectively [20]. We proposed a critical angle formulation that is simpler than (1) and it is expressed in (2) and (3), as shown at the bottom of the next page, where $\gamma = (2\alpha_{02}\beta_{02})/(\alpha_1\beta_1)$, and α_1 and β_1 are the effective attenuation and phase constants of the incidence plane wave, respectively [20]. To formulate these novel critical angle equations, we converted ζ_1 in (5) from [22] to $\xi_1 + \rho_1$ and performed some mathematical manipulation using several trigonometric identities, resulting in separation of ξ_1 from other terms. In addition, we considered the multivalued function property of the inverse cosine function, i.e., $\cos^{-1}(\cos\rho_1 - \gamma)$ could be $2\pi - \cos^{-1}(\cos\rho_1 - \gamma)$, leading to the two different solutions in (3). The conditions of nonuniform plane wave and media that create one or two critical angles are also presented in (2) and (3), respectively. These conditions were obtained by analyzing the range of $\xi_{c1}^{\zeta,\xi}$ and $\xi_{c2}^{\zeta,\xi}$ in (3). The condition in (2) equals $0 \leq \xi_{c1}^{\zeta,\xi} = \xi_{c2}^{\zeta,\xi} \leq 90°$ or $\xi_{c1}^{\zeta,\xi}$ satisfies $0 \leq \xi_{c1}^{\zeta,\xi} \leq 90°$, but $\xi_{c2}^{\zeta,\xi}$ does not satisfy $0 \leq \xi_{c2}^{\zeta,\xi} \leq 90°$, resulting in only one critical angle. On the other hand, the condition in (3) equals $\xi_{c1}^{\zeta,\xi} \neq \xi_{c2}^{\zeta,\xi}$ and not only $0 \leq \xi_{c1}^{\zeta,\xi} \leq 90°$ but also $0 \leq \xi_{c2}^{\zeta,\xi} \leq 90°$, leading to two different critical angles. Equations (2) and (3) can be used regardless of whether each medium is lossy or lossless and return the same results as (1) when the first medium is lossy because all of those equations are derived from [22, eq. (5)].

B. Determination of Correct Refraction Angles ζ_2 and ξ_2

1) Case Where $\rho_1 \leq 0$ or $\alpha_{02}\beta_{02} \neq \alpha_1\beta_1\cos^2(\rho_1/2)$: To calculate the correct refraction angles ζ_2 and ξ_2, first, $\xi_1^{\zeta,\xi}$ should be determined, whether it is ξ_1^{ζ} or ξ_1^{ξ}, because ξ_1^{ζ} and ξ_1^{ξ} have the same analytic expression [22]. It can be determined using [22, eq. (10)]. After determining ξ_1^{ζ} or ξ_1^{ξ}, based on the results of [12], [20], [21], [22], ζ_2 and ξ_2 can be computed from the following expressions when only one ξ_1^{ζ} or ξ_1^{ξ} exists:

$$\zeta_2 = \begin{cases} \sin^{-1}\left(\dfrac{\alpha_1\sin\zeta_1}{\alpha_2}\right), & \text{for } \xi_1 \leq \xi_1^{\zeta} \quad (4\text{-}1)\\ 180° - \sin^{-1}\left(\dfrac{\alpha_1\sin\zeta_1}{\alpha_2}\right), & \text{for } \xi_1 > \xi_1^{\zeta} \quad (4\text{-}2)\end{cases}$$

$$\xi_2 = \begin{cases} \sin^{-1}\left(\dfrac{\beta_1\sin\xi_1}{\beta_2}\right), & \text{for } \xi_1 \leq \xi_1^{\xi} \quad (5\text{-}1)\\ 180° - \sin^{-1}\left(\dfrac{\beta_1\sin\xi_1}{\beta_2}\right), & \text{for } \xi_1 > \xi_1^{\xi} \quad (5\text{-}2)\end{cases}$$

where α_1, β_1, ζ_1, and ξ_1 are known variables, and α_2 and β_2 can be computed from [20, eqs. (14) and (13)], respectively.

Baccarelli et al. [23] demonstrated the coexistence of two ξ_1^{ζ} or ξ_1^{ξ}. For this circumstance, ζ_2 and ξ_2 can be calculated from the following expressions:

$$\zeta_2 = \begin{cases} \sin^{-1}\left(\dfrac{\alpha_1\sin\zeta_1}{\alpha_2}\right), & \text{for } \xi_1 \leq \xi_{c1}^{\zeta} \text{ or } \xi_1 \geq \xi_{c2}^{\zeta}\\ 180° - \sin^{-1}\left(\dfrac{\alpha_1\sin\zeta_1}{\alpha_2}\right), & \text{for } \xi_{c1}^{\zeta} < \xi_1 < \xi_{c2}^{\zeta}\end{cases} \quad (6)$$

$$\xi_2 = \begin{cases} \sin^{-1}\left(\dfrac{\beta_1\sin\xi_1}{\beta_2}\right), & \text{for } \xi_1 \leq \xi_{c1}^{\xi} \text{ or } \xi_1 \geq \xi_{c2}^{\xi}\\ 180° - \sin^{-1}\left(\dfrac{\beta_1\sin\xi_1}{\beta_2}\right), & \text{for } \xi_{c1}^{\xi} < \xi_1 < \xi_{c2}^{\xi}\end{cases} \quad (7)$$

2) Case Where $\rho_1 > 0$ and $\alpha_{02}\beta_{02} = \alpha_1\beta_1\cos^2(\rho_1/2)$: When $\rho_1 > 0$ and $\alpha_{02}\beta_{02} = \alpha_1\beta_1\cos^2(\rho_1/2)$, i.e., $\xi_{c1}^{\zeta,\xi} = \xi_{c2}^{\zeta,\xi}$, the refraction angle reaches 90° at the critical angle, and it decreases right after this critical angle as ξ_1 increases (see [23, Fig. 8]). To prove this, let us consider a situation where $\alpha_1 = \alpha_1 + \varepsilon$, in which ε is a very small arbitrary positive constant. Then, the condition in (3) is satisfied and there exist two different critical angles. Also, these two critical angles have values that satisfy $\xi_{c1}^{\zeta,\xi} < \xi_1^{\zeta,\xi}$ with exact $\alpha_1 < \xi_{c2}^{\zeta,\xi}$. On the other hand, when $\alpha_1 = \alpha_1 - \varepsilon$, all conditions in (2) and (3) are not satisfied and there is no critical angle. In this case, the continuity of the solution requires two ξ_1^{ζ} or ξ_1^{ξ}, not one ξ_1^{ζ} and ξ_1^{ξ}, when $\alpha_1 = \alpha_1 + \varepsilon$. In other words, when exact α_1 is considered, the continuity of the solution requires the refraction angle to decrease right after the critical angle as ξ_1 increases. As a result, ζ_2 and ξ_2 can be computed from (4-1) and (5-1), respectively, regardless of whether ξ_1 is smaller or larger than $\xi_1^{\zeta,\xi}$.

III. Novel Critical Angle Formulation of 3-D Case

A. Critical Angle Formulation

When incident propagation vectors $\vec{\alpha}_1$ and $\vec{\beta}_1$ and the unit vector normal to the interface $\hat{z}$ are noncoplanar, the phase matching condition at the interface satisfies the following conditions [20]:

$$\alpha_1 \sin\zeta_1 = \alpha_2 \sin\zeta_2 \quad (8)$$
$$\beta_1 \sin\xi_1 = \beta_2 \sin\xi_2 \quad (9)$$

where the angles ζ_1, ζ_2, ξ_1, and ξ_2 are shown in Fig. 2. Furthermore, we derive two more equations [12] using the Adler–Chu–Fano formulation from [27]

$$\alpha_2^2 - \beta_2^2 = \alpha_{02}^2 - \beta_{02}^2 \quad (10)$$
$$\alpha_2\beta_2\cos\rho_2 = \alpha_{02}\beta_{02} \quad (11)$$

where angle ρ_2 is shown in Fig. 2. To calculate ξ_1^{ξ}, we impose $\xi_2 = 90°$ for all equations. Then, by performing some algebraic

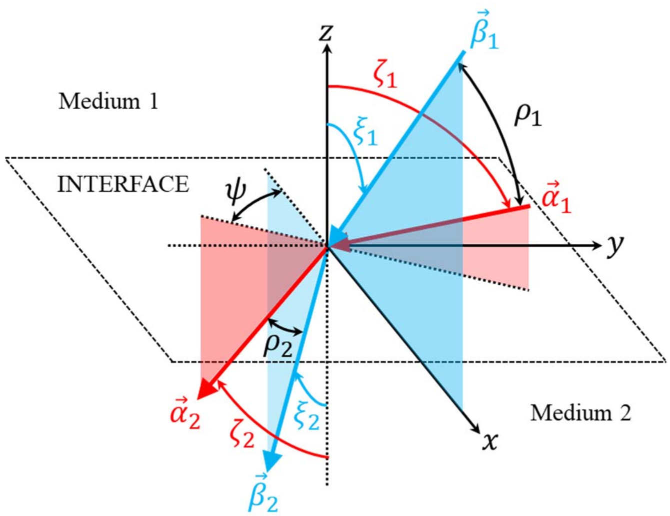

Fig. 2. Incidence and refraction of the nonuniform plane wave on the planar interface between two isotropic homogeneous possibly lossy media when $\vec{\alpha}_1$ and $\vec{\beta}_1$ and the unit vector normal to the interface $\hat{z}$ are noncoplanar, i.e., the 3-D case.

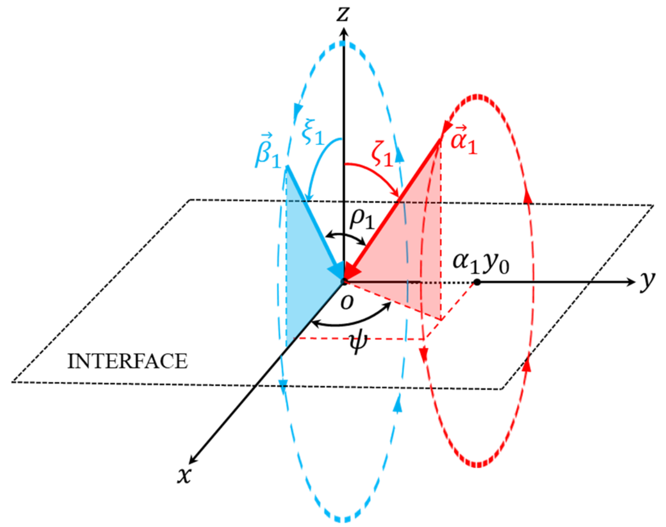

Fig. 3. Routes of incident propagation vectors $\vec{\alpha}_1$ and $\vec{\beta}_1$ when ρ_1 and y_0 are constants.

manipulations with (8), (9), (11), and [20, eq. (21)], we derive the following equation:

$$\sin \xi_1^{\xi} = \frac{\alpha_{02}\beta_{02}}{\alpha_1\beta_1 \sin \zeta_1^{\xi} \cos \psi^{\xi}} \tag{12}$$

where ζ_1^{ξ} and ψ^{ξ} represent ζ_1 and ψ when $\xi_2 = 90°$, respectively. As explained in Section II-B, the formulation of ζ_1^{ξ} and ξ_1^{ζ} possesses the same form for the 2-D case. By performing similar algebra as that which yielded (12), after imposing $\zeta_2 = 90°$, we discovered that the formulations of ξ_1^{ζ} and ξ_1^{ξ} have the same form not only for the 2-D case but also for the 3-D case. It means

$$\sin \xi_1^{\zeta,\xi} = \frac{\alpha_{02}\beta_{02}}{\alpha_1\beta_1 \sin \zeta_1^{\zeta,\xi} \cos \psi^{\zeta,\xi}} \tag{13}$$

where ζ_1^{ζ} and ψ^{ζ} represent ζ_1 and ψ when $\zeta_2 = 90°$. Inserting [20, eq. (20)] into (13) leads to the following:

$$\cos \xi_1^{\xi,\zeta} \cos \zeta_1^{\xi,\zeta} = \cos \rho_1 - \frac{\alpha_{02}\beta_{02}}{\alpha_1\beta_1}. \tag{14}$$

Now, we set ρ_1 and $y_0 = \sin \zeta_1 \sin \psi$ as constants. Then, the routes of incident propagation vectors $\vec{\alpha}_1$ and $\vec{\beta}_1$ would become, as shown in Fig. 3. Furthermore, by performing some algebra with $\cos \rho_1 = \hat{\alpha}_1 \cdot \hat{\beta}_1$, we obtain the following expression:

$$\cos \xi_1^{\zeta,\xi} \cos \zeta_1^{\zeta,\xi} = \cos \rho_1 \pm \sqrt{1 - y_0^2 - \cos^2 \zeta_1^{\zeta,\xi}} \sin \xi_1^{\zeta,\xi}. \tag{15}$$

After performing some algebra with (14) and (15), we finally formulate the critical angle equation as (16), where $A = \cos \rho_1 - (2\alpha_{02}\beta_{02})/(\alpha_1\beta_1)$ and $B = 1 - y_0^2$

$$\xi_1^{\zeta,\xi} = \cos^{-1} \sqrt{\frac{A \cos \rho_1 \pm \sqrt{\left(A^2 - B\right)\left(\cos^2 \rho_1 - B\right)}}{2B} + 0.5}. \tag{16}$$

B. Choice of Correct Sign

Equation (16) contains a positive–negative sign inside the square root; therefore, the correct sign should be chosen. A reason why this sign appears is because of the existence of two most possible cases for the relative position of $\vec{\alpha}_1$ and $\vec{\beta}_1$ satisfying the same constants ρ_1 and y_0. Fig. 4 reveals the possible cases of relative position between $\vec{\alpha}_1$ and $\vec{\beta}_1$, where $\vec{\alpha}_{p1}$ and χ_1 represent $\vec{\alpha}_1$ projected on the xz plane and the angle between the $+z$-axis and $-\vec{\alpha}_{p1}$, respectively. The possible three cases of relative position of $\vec{\alpha}_{p1}$ and $\vec{\beta}_1$ are $(\chi_1 < \xi_1)$, $(\chi_1 > \xi_1)$, and $(\chi_1 = \xi_1$ or $\vec{\alpha}_{p1} = 0)$. Each case can be easily distinguished, considering whether the y-component of $\hat{\alpha}_1 \times \hat{\beta}_1$ is positive, negative, or zero. The y-component of $\hat{\alpha}_1 \times \hat{\beta}_1$ can be represented as δ in (17) when $\xi_1 \in (0, 90°]$

$$\delta = \frac{\cos \zeta_1 - \cos \xi_1 \cos \rho_1}{\sin \xi_1}. \tag{17}$$

The correct sign can be determined by selecting the one satisfying the following conditions.

1) Case Where $\delta > 0$ or $\delta < 0$: Fig. 4(a) and (b) shows the cases where δ is positive and negative, respectively. If $|\xi_1 - \chi_1|$ is the same as in Fig. 4(a) and (b), the circumstances represented in Fig. 4(a) and (b) could have the same ρ_1 and y_0. Therefore, we must choose the appropriate sign in (16) considering whether the relative

$$\xi_1^{\zeta,\xi} = \frac{\cos^{-1}\left(\cos\rho_1 - \gamma\right) - \rho_1}{2}, \quad \text{for } (0 \le \alpha_{02}\beta_{02} < \alpha_{01}\beta_{01})\ or\ (\rho_1 \le 0\ and\ \alpha_{01}\beta_{01} = \alpha_{02}\beta_{02})\ or\ \left(\rho_1 > 0\ and\ \alpha_{02}\beta_{02} = \alpha_1\beta_1 \cos^2 \frac{\rho_1}{2}\right) \tag{2}$$

$$\xi_1^{\zeta,\xi} : \begin{cases} \xi_{c1}^{\zeta,\xi} = \dfrac{\cos^{-1}\left(\cos\rho_1 - \gamma\right) - \rho_1}{2} \\ \xi_{c2}^{\zeta,\xi} = \pi - \dfrac{\cos^{-1}\left(\cos\rho_1 - \gamma\right) + \rho_1}{2} \end{cases}, \text{for } \rho_1 > 0\ and\ \alpha_{01}\beta_{01} \le \alpha_{02}\beta_{02} < \alpha_1\beta_1 \cos^2 \frac{\rho_1}{2} \tag{3}$$

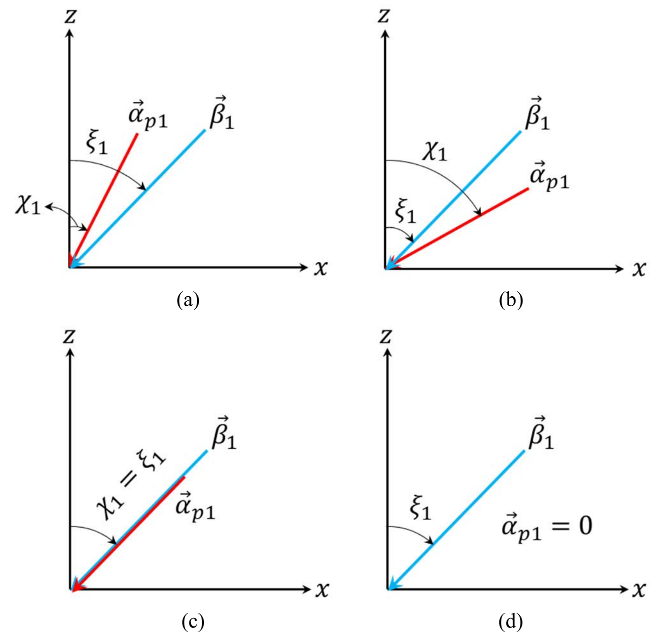

Fig. 4. Possible case of relative position between $\vec{\alpha}_{p1}$ and $\vec{\beta}_1$: (a) $\chi_1 < \xi_1$, (b) $\chi_1 > \xi_1$, (c) $\chi_{\alpha_1} = \xi_1$, and (d) $\vec{\alpha}_{p1} = 0$.

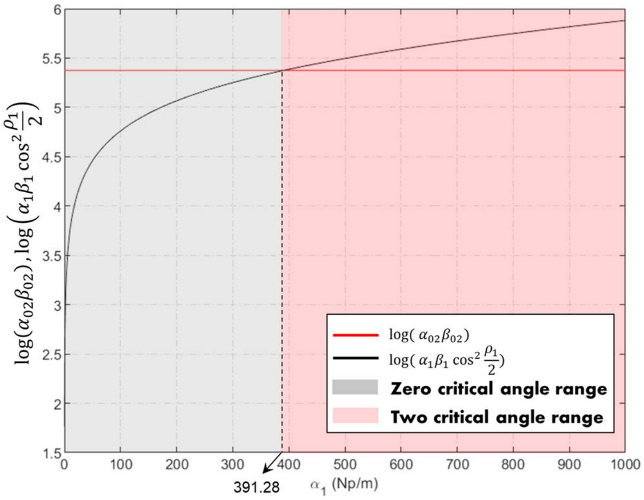

Fig. 5. Number of critical angles derived from the conditions in (2) and (3) when $f = 10$ GHz, $\varepsilon_{r1} = 30, \varepsilon_{r2} = 1, \mu_{r1} = 1, \mu_{r2} = 1, \sigma_1 = 1e-6$ S/m, $\sigma_2 = 6$ S/m, and $\rho_1 > 0$, while α_1 varies from 0 to 1000 Np/m.

position between $\vec{\alpha}_{p1}$ and $\vec{\beta}_1$ satisfies $\chi_1 < \xi_1$ or $\chi_1 > \xi_1$, i.e., $\delta > 0$ or $\delta < 0$. For the case where $\delta > 0$, the sign satisfying (18) should be chosen. For the case where $\delta < 0$, the sign satisfying (19) should be chosen

$$\sin^2\xi_1^{\zeta,\xi}\cos\rho_1 > \frac{\alpha_{02}\beta_{02}}{\alpha_1\beta_1} \tag{18}$$

$$\sin^2\xi_1^{\zeta,\xi}\cos\rho_1 < \frac{\alpha_{02}\beta_{02}}{\alpha_1\beta_1}. \tag{19}$$

Equations (18) and (19) are equivalent to the case where δ is positive and negative, respectively, when $\xi_1^{\zeta,\xi} \in (0, 90°)$. When $\xi_1^{\zeta,\xi} = 0$, a second medium must be lossless according to (16). If this were true and the incident wave was a nonuniform plane wave, a critical angle $\xi_1^{\zeta} = 0$ would always exist regardless of whether δ is positive or negative because $\xi_1 = 0$ means $\xi_2 = 0$, and ρ of nonuniform plane wave in the lossless medium is always 90° [20].

There is a possibility that both positive and negative (16) simultaneously satisfy (18) or (19), which means that two critical angles can exist for the 3-D case as well as the 2-D case. In this case, two $\xi_1^{\zeta,\xi}$ would be called $\xi_{c1}^{\zeta,\xi}$ and $\xi_{c2}^{\zeta,\xi}$, respectively, as in the 2-D case.

2) Case Where $\delta = 0$: Fig. 4(c) and (d) shows the cases where δ equals zero. In this case, $\cos^2\rho_1 - B$ in (16) becomes zero. Hence, the positive–negative sign becomes meaningless, and $\xi_1^{\zeta,\xi}$ is simplified as follows:

$$\xi_1^{\zeta,\xi} = \cos^{-1}\sqrt{\frac{A\cos\rho_1}{2B} + 0.5}. \tag{20}$$

C. Determination of Correct Refraction Angles ζ_2 and ξ_2

1) Case Where $\delta \neq 0$: Similar to the 2-D case, first, $\xi_1^{\zeta,\xi}$ should be determined, whether it is ξ_1^{ζ} or ξ_1^{ξ}, to compute the correct ζ_2 and ξ_2 because ξ_1^{ζ} and ξ_1^{ξ} have the same analytic expression, as explained in Section III-A. Moreover, [22, eq. (10)] can be used in this determination for not only the 2-D case but also for the 3-D case. After ξ_1^{ζ} or ξ_1^{ξ} is determined, the refraction angles can be calculated. Based on the result of [20], ζ_2 and ξ_2 can be calculated from the following expressions when only one ξ_1^{ζ} or ξ_1^{ξ} exists:

$$\zeta_2 = \begin{cases} \cos^{-1}\left(\sqrt{\cos^2\zeta_2}\right), & \text{for}\,\xi_1 \le \xi_1^{\zeta} \\ 180° - \cos^{-1}\left(\sqrt{\cos^2\zeta_2}\right), & \text{for}\,\xi_1 > \xi_1^{\zeta} \end{cases} \tag{21}$$

$$\xi_2 = \begin{cases} \cos^{-1}\left(\sqrt{\cos^2\xi_2}\right), & \text{for}\,\xi_1 \le \xi_1^{\xi} \\ 180° - \cos^{-1}\left(\sqrt{\cos^2\xi_2}\right), & \text{for}\,\xi_1 > \xi_1^{\xi} \end{cases} \tag{22}$$

where $\cos^2\zeta_2$ and $\cos^2\xi_2$ can be computed using [20, eqs. (22) and (23)]. Furthermore, when two ξ_1^{ζ} or ξ_1^{ξ} exist, ζ_2 and ξ_2 follow:

$$\zeta_2 = \begin{cases} \cos^{-1}\left(\sqrt{\cos^2\zeta_2}\right), & \text{for } \xi_1 \le \xi_{c1}^{\zeta} \text{ or } \xi_1 \ge \xi_{c2}^{\zeta} \\ 180° - \cos^{-1}\left(\sqrt{\cos^2\zeta_2}\right), & \text{for } \xi_{c1}^{\zeta} < \xi_1 < \xi_{c2}^{\zeta} \end{cases} \tag{23}$$

$$\xi_2 = \begin{cases} \cos^{-1}\left(\sqrt{\cos^2\xi_2}\right), & \text{for } \xi_1 \le \xi_{c1}^{\xi} or \xi_1 \ge \xi_{c2}^{\xi} \\ 180° - \cos^{-1}\left(\sqrt{\cos^2\xi_2}\right), & \text{for } \xi_{c1}^{\xi} < \xi_1 < \xi_{c2}^{\xi} \end{cases} \tag{24}$$

where $\xi_{c1}^{\zeta,\xi}$ is smaller $\xi_1^{\zeta,\xi}$ and $\xi_{c2}^{\zeta,\xi}$ is larger $\xi_1^{\zeta,\xi}$ among two $\xi_1^{\zeta,\xi}$.

2) Case Where $\delta = 0$: When $\delta = 0$, i.e., the positive–negative sign in (16) becomes meaningless and $\xi_1^{\zeta,\xi}$ converges to (20), there is a possibility that the refraction angle decreases right after the critical angle as ξ_1 increases so that (21) and (22) in determination procedure 1 cannot be used. This phenomenon is the same as one that is explained in the 2-D case refraction angle determination procedure 2 in Section II-B. However, the exact condition that causes this phenomenon for the 3-D case is difficult to deal with because, unlike the 2-D case, the conditions that produce one or two critical angles for the 3-D case are not discovered in this communication. It is rather complicated and authors leave it for future work. Nonetheless, an approximate refraction angle that is practically the same with the exact value can be obtained by conducting determination procedure 1 after calculating $\xi_1^{\zeta,\xi}$ using (16) with $y_0 = y_0 - \varepsilon$, where ε is a very small arbitrary positive constant.

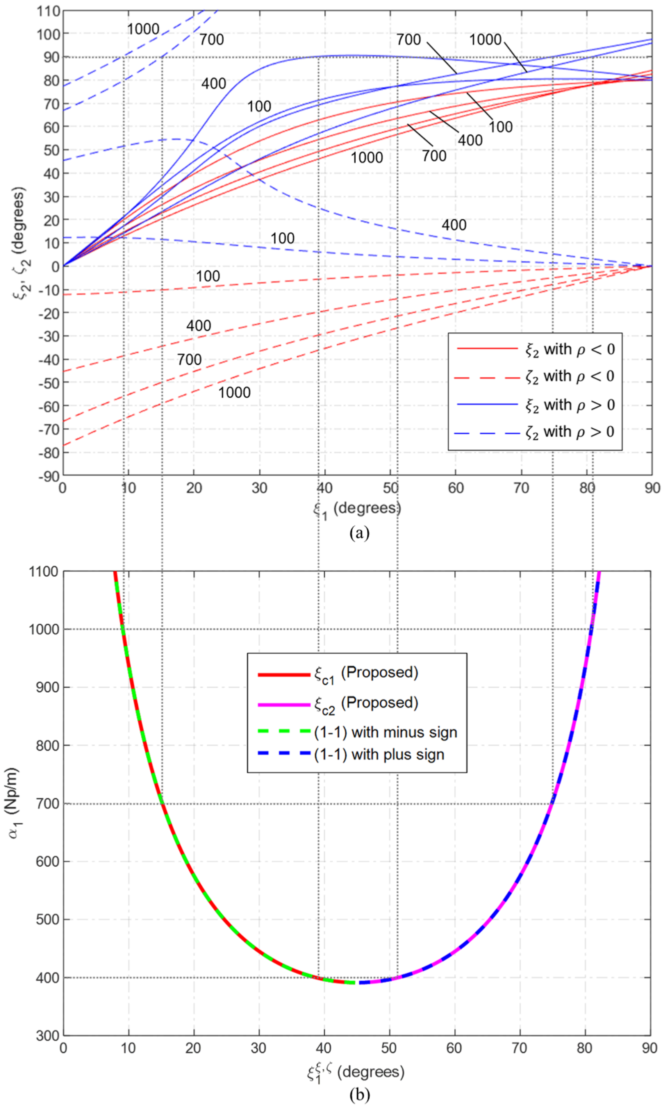

Fig. 6. Validation of the proposed 2-D critical angle formulation: (a) ζ_2 and ξ_2 as ξ_1 varies from 0.1° to 90° in increments of 0.1°, $\rho_1 < 0$ or $\rho_1 > 0$ and α_1 takes the values of 100, 400, 700, and 1000 Np/m; and (b) α_1 as $\xi_1^{\zeta,\xi}$ varies from 0° to 90° in increments of 0.1° for $\rho_1 > 0$.

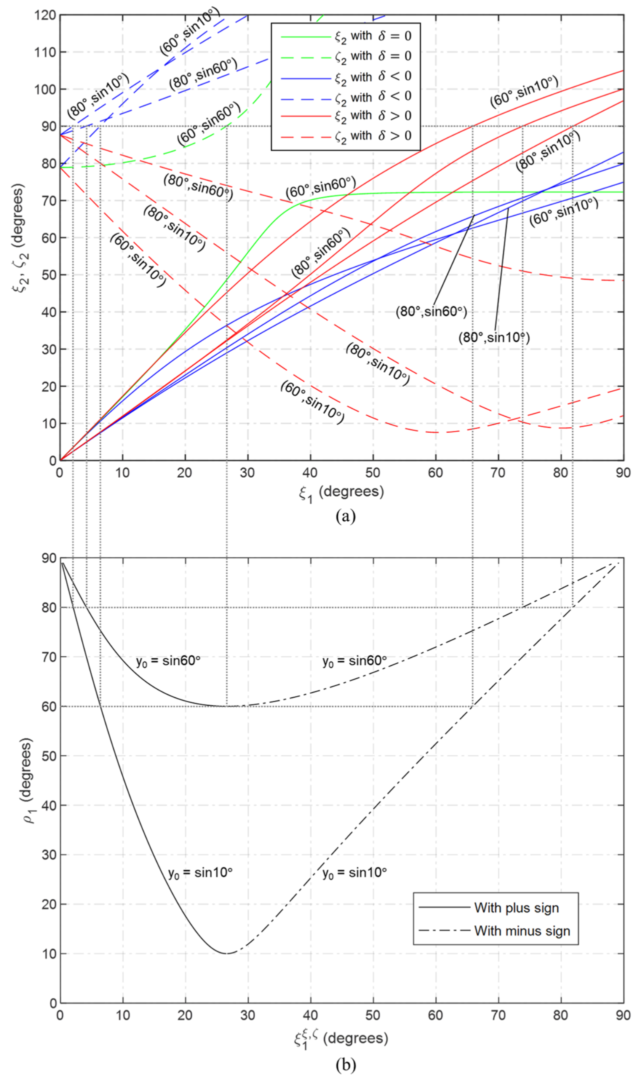

Fig. 7. Validation of proposed 3-D critical angle formulation: (a) ζ_2 and ξ_2 as ξ_1 varies from 0.1° to 90° in increments of 0.1°, and ρ_1 and y_0 take the values 60° and 80° and sin10° and sin60°, respectively, and (b) ρ_1 as $\xi_1^{\zeta,\xi}$ varies from 0° to 90° in increments of 0.1°, and y_0 takes the values of sin10° and sin60°.

IV. Validation

A. 2-D Case

Fig. 5 shows the number of critical angles when $f = 10$ GHz, $\varepsilon_{r1} = 30, \varepsilon_{r2} = 1, \mu_{r1} = 1, \mu_{r2} = 1, \sigma_1 = 1e-6$ S/m, $\sigma_2 = 6$ S/m, and $\rho_1 > 0$, as α_1 is varied from 0 to 1000 Np/m. Notably, $\alpha_{01}\beta_{01} \ll \alpha_{02}\beta_{02}$ due to the very low σ_1. When $\alpha_1 < \sim$391.28 Np/m, $\alpha_{01}\beta_{01}, \alpha_{02}\beta_{02}$, and $\alpha_1\beta_1\cos^2(\rho_1/2)$ do not satisfy any condition in (2) and (3), leading to no critical angle. On the other hand, when $\alpha_1 > \sim$391.28 Np/m, the condition in (3) is satisfied, resulting in two critical angles.

Fig. 6 presents the validation of the proposed critical angle formulation for the 2-D case when the frequency and electrical properties are the same as that in Fig. 5. Fig. 6(a) shows ζ_2 and ξ_2 when $\rho_1 < 0$ or $\rho_1 > 0$, with $\alpha_1 = 100$, 400, 700, and 1000 Np/m, as ξ_1 is varied from 0.1° to 90° in increments of 0.1°, using the refraction angle calculation procedure in Section II. (Here, the fundamental calculation procedure of refraction angle is the same as that of [20], [21], [22], [23], except the usage of (2) and (3) rather than (1) for critical angle equation.)

Fig. 6(b) shows α_1 when $\rho_1 > 0$, with the frequency and electrical properties mentioned above, as $\xi_1^{\zeta,\xi}$ is varied from 0° to 90° in increments of 0.1° and both $\xi_{c1}^{\zeta,\xi}$ and $\xi_{c2}^{\zeta,\xi}$ in (3), i.e., proposed formulation, are considered. In addition, in order to ensure the validity of the proposed critical angle formulation, $\xi_1^{\zeta,\xi}$ in (1), i.e., extant formulation, is also shown. The vertical lines are drawn from points where ζ_2 or ξ_2 in Fig. 6(a) becomes 90° to the line in Fig. 6(b). We can see that the values of α_1 where the vertical lines and the line in Fig. 6(b) intersect perfectly concur with α_1 of each line in Fig. 6(a), which validates the proposed critical angle formulation. Moreover, two critical angles exist when $\rho_1 > 0$ and $\alpha_1 = 400$ or 700 or 1000 Np/m, and no critical angle exists when $\rho_1 > 0$ and $\alpha_1 = 100$ Np/m, as expected from Fig. 5. Furthermore, as can be expected, no critical angle exists when $\rho_1 < 0$ because $\alpha_{01}\beta_{01} \ll \alpha_{02}\beta_{02}$, so that any conditions in (2) and (3) are not satisfied.

B. 3-D Case

Fig. 7 shows the validation of the proposed critical angle formulation for the 3-D case when $f = 10$ GHz, $\varepsilon_{r1} = 8, \varepsilon_{r2} = 1$,

$\mu_{r1} = 4, \mu_{r2} = 1, \sigma_1 = 5$ S/m, and $\sigma_2 = 4$ S/m, i.e., both media are lossy. Fig. 7(a) shows ζ_2 and ξ_2 when $\rho_1 = 60°$ or $80°$, with $y_0 = sin\ 10°$ or $sin\ 60°$, as ξ_1 varies from $0.1°$ to $90°$ in increments of $0.1°$, using the refraction angle calculation procedure in Section III. Numbers in brackets next to lines represent ρ_1 and y_0 pair. Except for the case where $\rho_1 = 60°$ and $y_0 = sin\ 60°$ pair is considered, i.e., $\delta = 0$, both conditions that $\delta > 0$ and $\delta < 0$ were considered for every pair. Fig. 7(b) shows ρ_1 when $y_0 = \sin 10°$ or $\sin 60°$, with the frequency and electrical properties mentioned above, as $\xi_1^{\zeta,\xi}$ varies from $0°$ to $90°$ in increments of $0.1°$ using (16) considering both positive–negative signs. The vertical lines are drawn from points where ζ_2 or ξ_2 in Fig. 7(a) becomes $90°$ to the lines in Fig. 7(b), which match y_0 of each line in Fig. 7(a). As observed in the figures, the values of ρ_1 in Fig. 7(b) where the vertical lines and lines in Fig. 7(b) intersect perfectly concur with ρ_1 of each line in Fig. 7(a), which validates the proposed formulation.

V. Conclusion

Novel critical angle equations essential for the determination of the correct refraction angles of nonuniform plane waves were formulated. For the 2-D case, a critical angle equation that is simpler than the one in a previous study, and under the conditions that one or two critical angles exist, is derived. The proposed 2-D critical angle equation can be used more efficiently in areas requiring massive computations, such as EM ray-tracing simulation. Furthermore, first, a 3-D critical angle equation was formulated. Consequently, the feasibility of utilization of the 3-D nonuniform plane wave refraction in various areas was confirmed. It will contribute to improving the accuracy of EM ray-tracing simulation and expanding EM theories related to nonuniform plane waves.

References

[1] F. Frezza and N. Tedeschi, "Electromagnetic inhomogeneous waves at planar boundaries: Tutorial," *J. Opt. Soc. Amer. A, Opt. Image Sci.*, vol. 32, pp. 1485–1501, 2015.

[2] A. Sommerfeld, "Über die ausbreitung der wellen in der drahtlosen telegraphie," *Ann. Physik*, vol. 333, pp. 665–736, Jan. 1909.

[3] J. Zenneck, "Über die fortpflanzung ebener elektromagnetischer wellen längs einer ebenen Leiterfläche und ihre beziehung zur drahtlosen telegraphie," *Annalen der Physik*, vol. 328, no. 10, pp. 846–866, 1907.

[4] R. M. Whitmer, "Fields in nonmetallic waveguides," *Proc. IRE*, vol. 36, no. 9, pp. 1105–1109, Sep. 1948.

[5] M. Muskat, "Potential distribution about an electrode on the surface of the Earth," *Physics*, vol. 4, no. 4, pp. 129–147, Apr. 1933.

[6] L. M. Brekhovskikh, *Waves in Layered Media*. New York, NY, USA: Academic, 1960.

[7] A. Otto, "Experimental investigation of surface polaritons on plane interfaces," in *Advances in Solid State Physics*, H. J. Queisser, Ed. New York, NY, USA: Pergamon, 1974.

[8] G. Goubau, "Surface waves and their application to transmission lines," *J. Appl. Phys.*, vol. 21, no. 11, pp. 1119–1128, 1950.

[9] D. R. Jackson and A. A. Oliner, "Leaky-wave antennas," in *Modern Antenna Handbook*, C. A. Balanis, Ed. Hoboken, NJ, USA: Wiley, 2008, ch. 7.

[10] Y. Wang, A. Helmy, and G. Eleftheriades, "Ultra-wideband optical leaky-wave slot antennas," *Opt. Exp.*, vol. 19, no. 13, pp. 12392–12401, 2011.

[11] A. Polemi and S. Maci, "A leaky-wave groove antenna at optical frequency," *J. Appl. Phys.*, vol. 112, no. 7, Oct. 2012, Art. no. 074320.

[12] R. D. Radcliff and C. A. Balanis, "Modified propagation constants for nonuniform plane wave transmission through conducting media," *IEEE Trans. Geosci. Remote Sens.*, vol. GRS-20, no. 3, pp. 408–411, Jul. 1982.

[13] N. Tedeschi and F. Frezza, "An analysis of the inhomogeneous wave interaction with plane interfaces," in *Proc. 31th URSI Gen. Assem. Sci. Symp. (URSI GASS)*, Aug. 2014, p. 109. [Online]. Available: https://ieeexplore.ieee.org/abstract /document/6929097

[14] R. Brem and T. F. Eibert, "A shooting and bouncing ray (SBR) modeling framework involving dielectrics and perfect conductors," *IEEE Trans. Antennas Propag.*, vol. 63, no. 8, pp. 3599–3609, Aug. 2015.

[15] Z. Cong, Z. He, and R. Chen, "An efficient volumetric SBR method for electromagnetic scattering from in-homogeneous plasma sheath," *IEEE Access*, vol. 7, pp. 90162–90170, 2019.

[16] Y. Huang, Z. Zhao, X. Li, Z. Nie, and Q.-H. Liu, "Volume equivalent SBR method for electromagnetic scattering of dielectric and composite objects," *IEEE Trans. Antennas Propag.*, vol. 69, no. 5, pp. 2842–2852, May 2021.

[17] X. M. Mitsalas, T. Kaifas, and G. A. Kyriacou, "Space and leaky wave radiation from highly lossy biological cylindrical human-limps models," *Prog. Electromagn. Res. B*, vol. 94, pp. 145–174, 2021.

[18] S. Perea-Puente and F. J. Rodríguez-Fortuño, "Complex wave-vectors in lossy materials: From polarisation-loss locking to bullseye metasurface," *Proc. SPIE*, vol. 12131, pp. 63–72, May 2022.

[19] C. A. Balanis, *Advanced Engineering Electromagnetics*. New York, NY, USA: Wiley, 1989.

[20] J. E. Roy, "New results for the effective propagation constants of nonuniform plane waves at the planar interface of two lossy media," *IEEE Trans. Antennas Propag.*, vol. 51, no. 6, pp. 1206–1215, Jun. 2003.

[21] F. Frezza and N. Tedeschi, "On the electromagnetic power transmission between two lossy media: Discussion," *J. Opt. Soc. Amer. A, Opt. Image Sci.*, vol. 29, no. 11, pp. 2281–2288, Nov. 2012.

[22] F. Frezza and N. Tedeschi, "Deeply penetrating waves in lossy media," *Opt. Lett.*, vol. 37, no. 13, pp. 2616–2618, Jul. 2012.

[23] P. Baccarelli, F. Frezza, P. Simeoni, and N. Tedeschi, "An analytical study of electromagnetic deep penetration conditions and implications in lossy media through inhomogeneous waves," *Materials*, vol. 11, no. 9, p. 1595, Sep. 2018.

[24] P. Baccarelli et al., "Verification of the electromagnetic deep-penetration effect in the real world," *Sci. Rep.*, vol. 11, no. 1, Aug. 2021, Art. no. 15928.

[25] S. Batool, F. Frezza, F. Mangini, and P. Simeoni, "Introduction to radar scattering application in remote sensing and diagnostics: Review," *Atmosphere*, vol. 11, no. 5, p. 517, May 2020.

[26] G. Solomakha et al., "A self-matched leaky-wave antenna for ultrahigh-field magnetic resonance imaging with low specific absorption rate," *Nature Commun.*, vol. 12, no. 1, p. 455, Jan. 2021.

[27] R. B. Adler, L. I. Chu, and R. M. Fano, *Electromagnetic Energy Transmission and Radiation*. New York, NY, USA: Wiley, 1960.